
Multidimensional Membership Mixture Models

Yun Jiang, Marcus Lim and Ashutosh Saxena

Department of Computer Science

Cornell University

Ithaca, NY 14850

{yunjiang, mk165, asaxena}@cs.cornell.edu

Abstract

We present the multidimensional membership mixture (M^3) models where every dimension of the membership represents an independent mixture model and each data point is generated from the selected mixture components jointly. This is helpful when the data has a certain shared structure. For example, three unique means and three unique variances can effectively form a Gaussian mixture model with nine components, while requiring only six parameters to fully describe it. In this paper, we present three instantiations of M^3 models (together with the learning and inference algorithms): infinite, finite, and hybrid, depending on whether the number of mixtures is fixed or not. They are built upon Dirichlet process mixture models, latent Dirichlet allocation, and a combination respectively. We then consider two applications: topic modeling and learning 3D object arrangements. Our experiments show that our M^3 models achieve better performance using fewer topics than many classic topic models. We also observe that topics from the different dimensions of M^3 models are meaningful and orthogonal to each other.

1 Introduction

Inherited from the mixture models' ability to approach complicated distribution using a small set of simpler distributions, topic models are used to capture 'topics'—distributions over the vocabulary—shared across different documents [8, 3, 41]. This concept has also been successfully applied to building image hierarchy [4, 23, 40, 24], where feature-object-scene relationships follow the word-topic-document analog.

Most previous models consider that a word is generated from one type of topic (which we call a single-dimensional membership). However, in some cases, an observation may be generated from two or multiple *types* of topics. As a pedagogical example, let us consider a case of Gaussian mixture modeling. Fig. 1 shows a dataset generated from 10 different Gaussian distributions, while we only need five *unique* means and two *unique* covariances. Unless we capture this effect—that the data is generated by two components from different parameter spaces—our model would not be parsimonious and thus susceptible to over-fitting. Such a scenario also happens in document modeling.

In this work, we present multidimensional membership mixture (M^3) models in which every data point has a multidimensional membership. Each dimension is a draw from an independent mixture model. As for the example above, we can use one mixture model for the means and another for the covariances. As a result, each point has a 2D membership. This leads to parsimonious representations when the data has a certain shared structure.

Now let us take topic modeling for the NIPS corpus⁵ as an example. Topics that the words are drawn from are the result of combining common topics (e.g., 'algorithm' and 'result') and session-specific topics (e.g., 'neural' and 'control').¹ Those topics are orthogonal in the sense of that papers of either

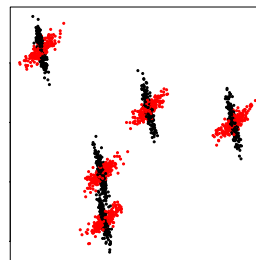


Figure 1: A mixture of ten Gaussians, with five unique means and two unique covariance matrices.

¹For simplicity, we use one keyword to represent a topic here.

neuroscience or control theory would have content about methods and results. Using M^3 models can not only obviate the need of unnecessary topics, but also identify such orthogonal structures in the data.

We can also view this multidimensional membership as a way of sharing parameters—observations assigned to different mixture components in one dimension may be assigned to the same component in another dimension and thus effectively share the parameters. This is different from hierarchical topic models, such as hierarchical DP [11, 41, 47]. Although they allow sharing among components branching from the same ancestors, the total number of components needed to model the data is not reduced accordingly.

Similar to other topic/mixture models, M^3 models need to infer latent membership for each data point. But the coupling of multiple mixture models through observed data makes inference more challenging. In this paper, we formulate and derive three instantiations of M^3 models: infinite M^3 , finite M^3 and hybrid M^3 , according to whether the number of mixture components is fixed or not. They are built upon multiple Dirichlet process mixture models (DPMMs), multiple latent Dirichlet allocation (LDA) models, and a combined DPMM and finite mixture model.

In the experiments, we first present a proof-of-concept example of applying the infinite M^3 model on the task of Gaussian mixture modeling. We then consider the task of document modeling. We compare our finite M^3 model with different topic models (including LDA, hierarchical DP, etc.) on several corpora. Extensive experiments show that our model achieves lower perplexity on the hold-out documents while having fewer topics than the baselines. The extracted topics from different the dimensions also reflect certain orthogonality.

Finally, we also consider the problem of learning 3D object arrangements (which is useful in scene understanding, object recognition and robotic applications). An object being at a particular place is governed by two orthogonal factors—its affordances (i.e., how it is used by humans such as drinking or touching) [29] and potential human poses (e.g., sitting in a chair or browsing a book shelf) [14, 10]. Therefore we use two independent mixture models and enable objects of different usages be associated with one human pose and vice versa. Results show that our hybrid M^3 model outperforms both finite and infinite mixture models whose mixture components are defined on the joint space of human poses and object affordances.

2 Related Work

There is a huge body of work employing mixture models. Here we only name a few in the area of probabilistic topic models. More recent developments in topic modeling can be found in [1, 39].

Most methods used to extract topics from a document corpus are grounded in latent variable models and statistical decomposition techniques, such as mixture of unigrams model [33] and probabilistic latent semantic indexing model (pLSI) [16]. Later, Blei et al. [3] proposed LDA to model the hierarchy of a corpus to allow different documents to share similar topic proportions and words from one document are sampled from the same topic distribution. It is later extended to nonparametric hierarchical models [11, 41, 47], so that the hierarchy and the number of topics are learned together. The inferential difficulty in those topic models can be alleviated by using variational inference [28, 3, 42] or MCMC sampling [31], including collapsed Gibbs sampling [12]. These models consider single-dimensional topics, and therefore are complementary our method.

Many models relax the assumptions in LDA by modeling word non-exchangeability [44, 13], or by modeling the correlations among topics [2, 20, 34]. These ideas are complementary to ours, and similar techniques may be applied to M^3 models. Further, there has also been work on incorporating other meta-data such as authors [36, 6], citations [30], and tags [7]. Our M^3 model does not require such meta-data. More importantly, none of these extensions consider the factorization of topics into multiple mixture models.

Topic model have been widely applied to computer vision applications such as building image hierarchy [23], object detection [40], activity recognition [46], classification, annotation and segmentation [24]. In some applications, the model is augmented with spatial information to yield spatially coherent topics [45]. However, none of the models presented in these works consider generation of data-points as a multi-dimensional mixture of topics.

There are previous works in matrix factorization [9], factored models [35] and parameter sharing [21, 17, 22, 27, 32], where a lower dimensional representation of the parameters is used. Even though these approaches are quite different from our M^3 models, they are relevant to our work since M^3 model also uses a compact “factored” representation for the parameters.

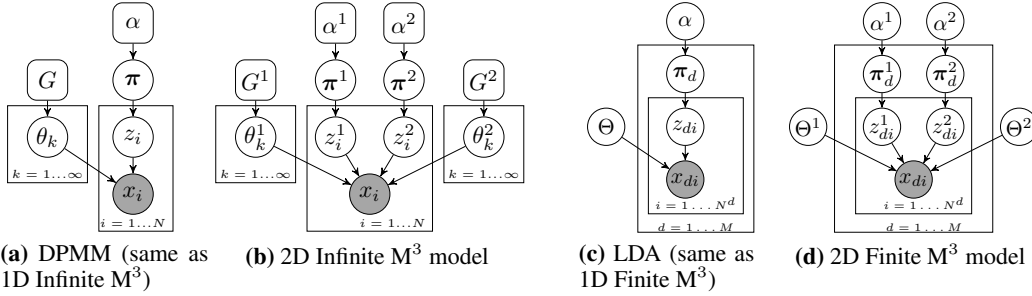


Figure 2: Two instantiations of our M^3 models: infinite and finite 2D M^3 models and their corresponding models in 1D.

Our model does not diverse far from multidimensional clustering [5], two-way groupings [37, 15] and some biclustering models [25]. However in this work, we are interested in modeling the posterior density and topics instead of clustering.

Many collaborative filtering methods are also built upon mixture models [19, 26], where user preferences are often modeled by different mixture components. This is similar to classic topic models whose membership is single-dimensional. The flexible mixture model [38] however considers 2D membership (user and object group) for an observed rating score. It is close to our work but we consider (Dirichlet) priors and infinite number of groups.

3 Multidimensional Membership Mixture (M^3) Models

We present the general idea of our approach in this section, and then describe three specific instantiations in the next section.

A mixture model typically consists of K mixture components, each of which is a distribution parameterized by θ_k , denoted as $F(\theta_k)$. Drawing a data point x involves choosing a mixture component $z \in \{1, \dots, K\}$ according to the mixing proportions $\pi = (\pi_1, \dots, \pi_K)$ (subject to $\sum_{k=1}^K \pi_k = 1$), and then drawing from $F(\theta_z)$, i.e.,

$$z|\pi \sim \pi; \quad x|z, \theta \sim F(\theta_z). \quad (1)$$

Depending on whether K is fixed or not, mixture models can be categorized as finite and infinite (or nonparametric) mixture models.

Our M^3 models assume data is generated *jointly* by several independent mixture models. Particularly, an L -dimensional M^3 model of L different mixture models, each having K^ℓ components parameterized by θ_k^ℓ . Now, generating a data point x involves choosing a mixture component $z^\ell \in \{1, \dots, K^\ell\}$ for *each* of the L dimensions. Given $\Theta = (\theta_k^\ell)_{k=1, \dots, K^\ell}^{\ell=1, \dots, L}$ and $\mathbf{z} = (z^1, \dots, z^L)$, we then draw x from the distribution parameterized by the selected L mixture components together:

$$z^\ell|\pi^\ell \sim \pi^\ell, \quad \forall \ell = 1, \dots, L; \quad x|\mathbf{z}, \Theta \sim F(\theta_{z^1}^1, \dots, \theta_{z^L}^L). \quad (2)$$

Note that the domain of the density function F is now a Cartesian product of the domains of L mixture models, which may or may not be the same.

M^3 models are related to the standard mixture models in the following ways. When $L = 1$, it degenerates to the standard mixture model. When $L > 1$, we can also cast it into an equivalent (single-dimensional) mixture model by defining a new mixture component for any combination of L components as $\theta'_{j_k} = (\theta_{j_1}^1, \dots, \theta_{j_L}^L)$ where $j_\ell \in \{1, \dots, K^\ell\}$. This leads to a total of $\prod_{\ell=1}^L K^\ell$ mixture components. When L or K^ℓ is large, the corresponding mixture model would be prohibitive to compute and may tend to over-fit the data. On the other hand, M^3 models only construct $\sum_{\ell=1}^L K^\ell$ mixture components. While this is much more parsimonious, our method relies on the assumption that the data is drawn from shared mixture components whose parameters are generated from independent processes. Our model would also be able to obtain better estimates of the parameters because now more observations would effectively be used for computation.

Note that an L -dimensional M^3 model is not the same as L independent mixture models, as they are *linked through the observations*. This coupling would result in challenges in the inference, such as when optimizing parameters of the L mixture models jointly or sampling from their joint posterior distribution. In the following sections, we will show how to derive and use some specific M^3 models.

4 Formulation and Inference for Three Instantiations of M^3 models

In this section, we describe our three specific instantiations of the M^3 model. Each is a combination of $L = 2$ mixture models, and we informally call them 2-D M^3 .² Experiments on each of these models will be presented in Section 5.

4.1 Infinite M^3 Models using Dirichlet Processes

When the number of components, K , is unknown, nonparametric Bayesian methods are often used. For example, Dirichlet process mixture model (DPMM), which is also referred as infinite mixture model, can adapt K to the data automatically (overview of DP can be found in [43]). DPMM can be constructed using a stick-breaking process:

$$\pi \sim \text{GEM}(1, \alpha) \quad \theta_k \sim G_0 \quad z_i | \pi \sim \pi \quad x_i | z_i, \theta_{1:\infty} \sim F(\theta_{z_i}) \quad (3)$$

where G_0 is the base distribution of θ and α is the concentration parameter. Chinese restaurant process provides another perspective to understand how z_i is selected:

$$z_i = z | z^{-i} = \begin{cases} \frac{n_z^{-i}}{N-1+\alpha} & \text{if } z \text{ is previously used} \\ \frac{\alpha}{N-1+\alpha} & \text{otherwise} \end{cases} \quad (4)$$

where superscript $-i$ denotes everything except the i^{th} instance and n_z^{-i} equals the number of data points assigned to the component z excluding x_i .

We formulate the 2-D infinite M^3 model as a combination of two DPMMs, as shown in Fig. 2b. Each DP mixture model follows the same stick-breaking process as in Eq. (3), except that x_i is now sampled as

$$x_i | z_i^1, z_i^2, \theta_{1:\infty}^1, \theta_{1:\infty}^2 \sim F(\theta_{z_i^1}^1, \theta_{z_i^2}^2). \quad (5)$$

We now define the conditional distribution for z_i^1, z_i^2 , the counterpart of Eq. (4) in our M^3 model. Let n_{cd}^{-i} equals the number of observations (excluding x_i) with $z_j^1 = c$ and $z_j^2 = d$. And let $n_{c \cdot}^{-i} = \sum_d n_{cd}^{-i}$ and $n_{\cdot d}^{-i} = \sum_c n_{cd}^{-i}$. If we assume z_i^1 and z_i^2 are independent, the joint conditional is decomposed into their own conditional same as Eq. (4) by replacing n_z^{-i} with $n_{z \cdot}^{-i}$ and $n_{\cdot z}^{-i}$. However, this is such a strong assumption that does not hold in general. Therefore, we introduce a *sharing parameter* $\omega \in [0, 1]$ to control the correlation between the two. We define the joint conditional as follows,³

$$z_i^1 = c, z_i^2 = d | z^{1,-i}, z^{2,-i} = \begin{cases} \frac{(1-\omega)n_{c \cdot}^{-i}n_{\cdot d}^{-i} + \omega n_{cd}^{-i}(N-1)}{(N-1)(N-1+\alpha)} & n_{c \cdot}^{-i} > 0 \text{ and } n_{\cdot d}^{-i} > 0 \\ \frac{\omega^1 \alpha n_{\cdot d}^{-i}}{(N-1)(N-1+\alpha)} & n_{\cdot d}^{-i} > 0 \\ \frac{\omega^2 \alpha n_{c \cdot}^{-i}}{(N-1)(N-1+\alpha)} & n_{c \cdot}^{-i} > 0 \\ \frac{\omega \alpha}{N-1+\alpha} & \text{otherwise} \end{cases} \quad (6)$$

with ω^1 and ω^2 (subject to $\omega + \omega^1 + \omega^2 = 1$) used to tune the relative concentration parameter between the two dimensions. Under this definition, ω constructs a smooth continuum between 2-D M^3 models and 1-D M^3 models (same as DPMM): when $\omega = 1$, z_i^1 and z_i^2 will always be equal and hence it simply boils down to a single DPMM; when $\omega = 0$, the equation above decomposes into two distributions similarly to Eq. (4) for z_i^1 and z_i^2 respectively.

We can use the algorithm of Gibbs sampling with auxiliary parameters [31] to sample $z^1, z^2, \Theta^1, \Theta^2$ from their posterior distributions:

1. For $i = 1, \dots, n$: sample z_i^1 and z_i^2 according to Eq. (6) multiplying $f(x_i | \theta_{z_i^1}^1, \theta_{z_i^2}^2)$;
2. For $l = 1, 2$: sample θ_k^l with the probability given by $G^l(\theta_k^l) \prod_{i: z_i^l = k} f(x_i | \theta_{z_i^1}^1, \theta_{z_i^2}^2)$.

Here $f(\cdot | \theta^1, \theta^2)$ is the density function of distribution $F(\theta^1, \theta^2)$.

Implementations of the second step differ depending on which F and $G^{1:2}$ are used. For example, finding conjugate priors for exponential family distributions is easy for M^3 , but it is not so when $G^{1:2}$ are both Dirichlet distributions because they are no longer the conjugate priors for a multinomial distribution F . In such cases, other methods based on sampling such as Metropolis-Hastings [31] or Gibbs sampling [12, 41] could be used depending on the distribution. In this paper, we will present a concrete example with F as a normal distribution and G is its conjugate prior in Section 5.1.

²Although we only present 2-D cases, generalization to $L > 2$ is straightforward.

³Note that the superscript in the symbols z, ω , etc. denotes the dimension ($\ell = 1, \dots, L$), not the exponent.

4.2 Finite M^3 Models for Topic Modeling

Latent Dirichlet allocation (LDA) employs a hierarchical finite mixture model to describe the generative process of a document: first, a topic proportion π over K topics is drawn from a symmetric Dirichlet distribution with prior α ; then a topic z_i is chosen for each word x_i , and x_i is drawn from θ_{z_i} , a multinomial distribution over the whole vocabulary of size V . Thus, LDA allows words from the same document share similar topic distributions while documents share finite topics. However in many real-world datasets, words could be generated from several different *types* of topics. In this section, we model each type of topic as a dimension in our M^3 model.

We define our 2-D finite M^3 model as follows (shown in Fig. 2d): we assume two independent topic spaces and a word is drawn from a topic synthesized by two topics—one from each topic space—with the probability of

$$p(x|\theta_{z^1}^1, \theta_{z^2}^2) = \frac{1+\omega}{2}\theta_{z^1, x}^1 + \frac{1-\omega}{2}\theta_{z^2, x}^2 \quad (7)$$

where $\omega \in [0, 1]$ tunes the weight of the two topic models in forming a new topic. It serves similar purpose as the ω in Eq. (6): the 2-D finite M^3 model degenerates to the classic LDA when $\omega = 1$.

Same as other topic models, the goal of applying finite M^3 model to corpora is density estimation, i.e., to maximize the likelihood of the test documents. After integrating out $\pi^{1:2}$ and $z^{1:2}$, we obtain the likelihood of a document $\mathbf{w} = (x_1, \dots, x_N)$ conditioned on the model as,

$$p(\mathbf{w}|\alpha^{1:2}, \Theta^{1:2}) \propto \int \int \left(\prod_{i=1}^{K^1} (\pi_i^1)^{\alpha^1 - 1} \right) \left(\prod_{i=1}^{K^2} (\pi_i^2)^{\alpha^2 - 1} \right) \times \prod_{i=1}^N \sum_{z^1}^{K^1} \sum_{z^2}^{K^2} \pi_{z^1}^1 \pi_{z^2}^2 \left(\frac{1+\omega}{2}\theta_{z^1, x_i}^1 + \frac{1-\omega}{2}\theta_{z^2, x_i}^2 \right) d\pi^1 d\pi^2. \quad (8)$$

This distribution is intractable to compute in general. We therefore approximate it using a variational inference similar to the one used in LDA [3].

Variational Inference. Following the classic LDA method, we use the variational distribution, $q(\pi^{1:2}, z^{1:2}|\gamma^{1:2}, \phi^{1:2}) = q(\pi^1|\gamma^1)q(\pi^2|\gamma^2)\prod_{n=1}^N q(z_n^1|\phi_n^1)q(z_n^2|\phi_n^2)$, as an approximation to the true posterior distribution $p(\pi^{1:2}, z^{1:2}|\mathbf{w}, \alpha^{1:2}, \Theta^{1:2})$. The difference between the two is quantified by the KL divergence:

$$D(q||p) = \log p(\mathbf{w}|\alpha^{1:2}, \Theta^{1:2}) - \mathcal{L}(\gamma^{1:2}, \phi^{1:2}; \alpha^{1:2}, \Theta^{1:2}). \quad (9)$$

Since KL divergence is always non-negative, \mathcal{L} above is the lower bound of $p(\mathbf{w}|\alpha^{1:2}, \beta^{1:2})$. Therefore, our goal is to maximize \mathcal{L} so that the likelihood $p(\mathbf{w}|\alpha^{1:2}, \beta^{1:2})$ can be large as well. During inference, the goal is to optimize \mathcal{L} with respect to $\phi^{1:2}$ and $\gamma^{1:2}$ for each document. This is similar to LDA and thus we provide details only in the supplementary material. During training, given D documents, our goal is to find the model's parameters that maximize \mathcal{L} . We solve it by iteratively inferring $(\phi_d^{1:2}, \gamma_d^{1:2})$ for each document \mathbf{w}_d and estimating $\alpha^{1:2}, \Theta^{1:2}$ and ω given the rest. The step of parameter estimation is more challenging than the classic LDA due to the entanglement of the two topics and the sharing parameter ω .

Parameter Estimation. When the variational distribution is fixed, the terms involving $\alpha^{1:2}$ in \mathcal{L} are as follows. Here, $\Gamma(\cdot)$ is the Gamma function, and $\Psi(\cdot)$ is the digamma function.

$$\mathcal{L}_{\alpha^{1:2}} = \sum_{t=1}^2 \left(\log \Gamma(K^t \alpha^t) - K^t \log \Gamma(\alpha^t) + (\alpha^t - 1) \sum_{i=1}^{K^t} \left(\Psi(\gamma_i^t) - \Psi\left(\sum_{j=1}^{K^t} \gamma_j^t\right) \right) \right). \quad (10)$$

Since α^1 and α^2 are independent to each other and to ω and $\Theta^{1:2}$ as well. We can update them separately, similar to LDA. However, the terms involving $\Theta^{1:2}$ and ω in \mathcal{L} are,

$$\mathcal{L}_{\Theta^{1:2}, \omega} = \sum_{d=1}^M \sum_{n=1}^{N_d} \sum_{i=1}^{K^1} \sum_{j=1}^{K^2} \phi_{dni}^1 \phi_{dnj}^2 \log \left(\frac{1+\omega}{2}\theta_{i, \mathbf{w}_{dn}}^1 + \frac{1-\omega}{2}\theta_{j, \mathbf{w}_{dn}}^2 \right). \quad (11)$$

Any derivative of this would have terms containing $2/((1+\omega)\theta_{i, \mathbf{w}_{dn}}^1 + (1-\omega)\theta_{j, \mathbf{w}_{dn}}^2)$ in the innermost summation, making it hard to obtain closed-form expressions. We instead convert the problem into an unconstrained problem, by defining the new objective function:

$$\text{minimize}_{\Theta^{1:2}, \omega} \quad -\mathcal{L}_{\Theta^{1:2}, \omega} + \frac{1}{2} \sum_{i=1}^{K^1} \lambda_i \left(\sum_{j=1}^V \theta_{ij}^1 - 1 \right)^2 + \frac{1}{2} \sum_{i=1}^{K^2} \eta_i \left(\sum_{j=1}^V \theta_{ij}^2 - 2 \right)^2, \quad (12)$$

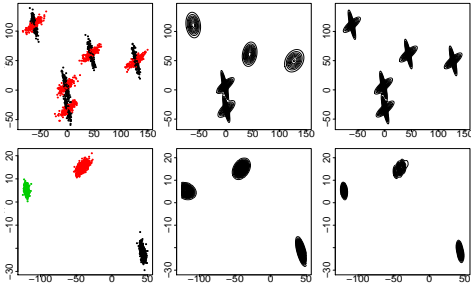


Figure 3: Given data generated from a mixture of Gaussian distributions (left), the density estimation obtained by the standard DPMM (middle) and our infinite M^3 model (right). Bottom row shows that even when there are no shared parameters, our model performs as well as the DPMM.

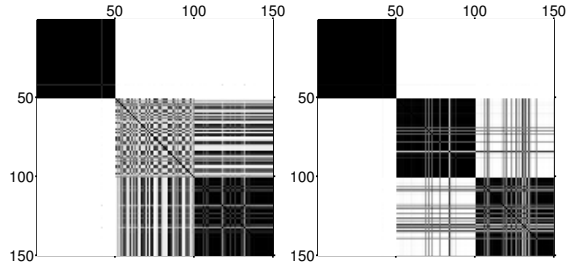


Figure 4: Confusion matrices for **Dataset-0** obtained by the DPMM (left) and infinite M^3 model (right). The intensity of each pixel represents the percentage of two flowers are grouped into one cluster. The ground-truth is a 3×3 block-diagonal matrix.

where $\{\lambda_i, \eta_i\}$ impose a positive penalty for violating the constraint. Each $\{\lambda_i, \eta_i\}$ is initialized with a small value and gradually increased when the corresponding constraint is violated. Given the weights, optimal $\Theta^{1:2}$ and ω are computed by the limited-memory BFGS algorithm, a standard quasi-Newton method. In practice, the penalties are only updated a few times before it converges.

4.3 Hybrid M^3 Models

There are many cases when one mixture model has a fixed number of components while the other one does not. For example, in the task of scene understanding, we can model object type and its pose separately. While objects can appear in countless poses, it is reasonable to assume a finite set of object categories. Therefore, we form our hybrid M^3 model as a combination of DPMM and a finite mixture model. We update the assignments z_i^1 and z_i^2 in turn. We use standard DP to sample z_i^1 given z_i^2 , and use maximum likelihood estimation to update z_i^2 given a set of sampled z_i^1 .

5 Applications and Experimental Results

In this section, we first illustrate how our M^3 models behaves on the task of Gaussian mixture modeling. Then we evaluate our finite M^3 model on the task of document modeling, on four different datasets and against three baselines. Finally, we apply our hybrid M^3 model to the task of estimating object arrangements in human environments.

5.1 Gaussian Mixture Model

In the classic Gaussian mixture model, data points are drawn from a set of different Gaussian distributions, i.e. $x_i|z_i, (\mu_1, \Sigma_1), \dots, (\mu_K, \Sigma_K) \sim N(\mu_{z_i}, \Sigma_{z_i})$, whereas our 2D M^3 model uses two mixture models for means and covariances respectively, and draws data from

$$x_i|z_i^1, z_i^2, \mu_1, \dots, \mu_{K^1}, \Sigma_1, \dots, \Sigma_{K^2} \sim N(\mu_{z_i^1}, \Sigma_{z_i^2}).$$

We use conjugate prior for μ and Σ (Gaussian and inverse Wishart distribution respectively), with same hyperparameters in both algorithms.

We created a synthetic dataset for evaluating the results in terms of density estimation. For our model, it is $x \sim \sum_c \sum_d p(c, d|z^1, z^2) \mathcal{N}(\mu_c, \Sigma_d)$ averaged over 1000 samples. From the contours shown in Fig. 3, we can see that our method successfully identifies correct clusters in both sharing and non-sharing cases. The averaged normalized mutual information (NMI) for our model is 0.75 and 0.96 compared to 0.66 and 0.97 of the DPMM.

We also tested it on the Iris dataset (**Dataset-0**) containing 150 flowers from three species with four features for each sample.⁴ The confusion matrices in Fig. 4 show that while both methods can correctly find the first species, DPMM is confused about the last two species. NMI of M^3 model is 0.72 versus 0.67 for the DPMM.

5.2 Document Topic Modeling

We test our finite M^3 model (tagged ‘FM3’ in the figures) on four document corpora: **Dataset-1** contains processed NIPS 1-12 proceedings with 1447 papers organized into 9 sections and 5270 words after removing words appeared more than 4000 times or fewer than 50 times;⁵ **Dataset-2** includes

⁴<http://archive.ics.uci.edu/ml/datasets/Iris>

⁵<http://www.gatsby.ucl.ac.uk/~ywteh/research/data.html>

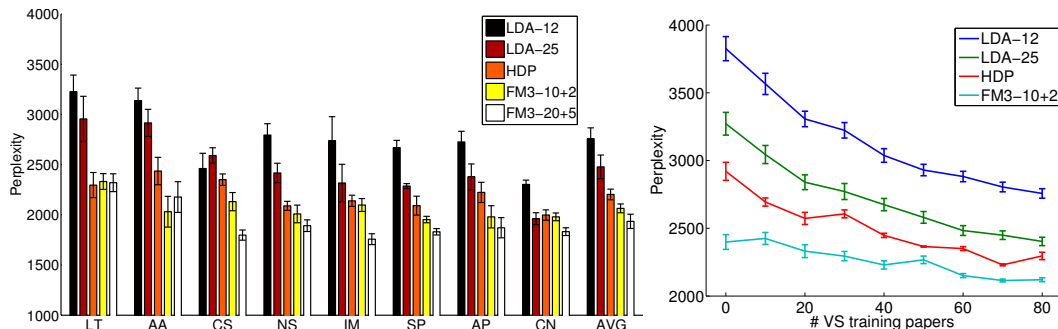


Figure 5: Results on Dataset-1. Perplexity of mixing VS and other 8 sections (left) and the average perplexity when changing the number of training documents from VS (right). The error bars are one standard error.

randomly selected 1000 documents from the 20 newsgroups with a total of 1498 words after removing stop-words and words in fewer than 5 documents;⁶ **Dataset-3** selects 1000 encyclopedia articles with 1200 words;⁷ **Dataset-4** takes 500 articles from Psychological Review with 1244 words.⁸ All the following results are based on 5 runs or 5-fold cross validation. Experiments on the first two datasets are in the same setup as in [41] and [47] respectively.

To investigate how well our model can learn general topics and section-specific topics, we train on 80 articles from the VS (vision science) section and 80 articles from one of the other 8 sections. We test on the rest 47 VS papers. We use the perplexity [3] of the on-hold documents to evaluate the learned topic model: $\text{perplexity}(\mathbf{w}_1, \dots, \mathbf{w}_D) = \exp(-(\sum_{d=1}^D \log p(\mathbf{w}_d)) / \sum_{d=1}^D N^d)$. A lower perplexity indicates higher likelihood of the test data and thus better performance.

Fig. 5-left shows the perplexity obtained by LDA, HDP and our method. In the comparison with LDA, we set the LDA’s topic number K equal to the total sum of topic numbers of M^3 model $K^1 + K^2$, so that the two models have the same number of parameters. We see that our method performs significantly better than LDA across all eight sections for both 12 and 25 topics. This is due to that M^3 model has effectively have more topics than LDA. Such trends hold for different values of K , K^1 and K^2 .

In presented results, we had set the second dimension of our M^3 model to have only a few topics ($K^2 = 2$ or 5). This enforces all documents from different sections have to ‘share’ them. Our method and HDP both outperform than LDA, showing that the ability of having shared topics is helpful. However, HDP does so in a hierarchy so that a sub-tree share similar topic proportions. It however does not reduce the number of topics needed to model. In fact, the number of topics used in HDP is around 55, far more than our 12 topics.

In another experiment on Dataset-1, we change the number of training documents from VS from 0 to 80, but always test on the rest 47 VS documents. When the number is small, the domain of the training and test dataset would be different and thus can be used to test the transfer of topic learning. Fig. 5-right shows the perplexity, averaged over all sections, with respect to different training documents. We can see that the performance of LDA largely depends on the number of VS papers, while the change in the perplexity of HDP and our model is less significant. Our finite M^3 method not only beats all the baselines but also gives the most consistent results in all cases. This demonstrates that 1) our model can learn the common topics of two different sections, and 2) it is less sensitive to having a small training set since the multi-dimensional membership effectively allows more documents to be used for estimating the parameters.

We also test on the other three datasets and the results are shown in Fig. 6. Compared to the baselines, our M^3 model obtains the lowest perplexity and demonstrates its robustness in different scenarios.

In order to explore what orthogonal topics our M^3 model discovered, we list one topic from each dimension in Fig. 7. Topics from the first row are quite different from each other containing some keywords for specific sections, such as ‘digits’ for the SP (speech and signal processing) while the topics in the bottom row are mostly from popular words in NIPS such as ‘work’ and ‘algorithms’. This indeed reflects that M^3 represents topics parsimoniously.

⁶<http://people.csail.mit.edu/jrennie/20Newsgroups/>

⁷<http://www.cs.nyu.edu/~roweis/data.html>

⁸http://psiexp.ss.uci.edu/research/programs_data/toolbox.htm

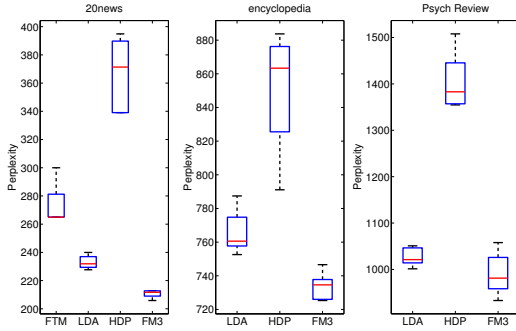


Figure 6: Results on **Dataset2-4**, performed by FTM (reported in [47]), LDA, HDP and our finite M^3 model. For LDA and FM3, we only report the best performance among different number of topics.

In M^3 models, setting K^1 and K^2 would affect the performance. Similar to LDA, the optimal value for the number of topics ($K^1 + K^2$) varies with the size and heterogeneity of the corpus, and may to try different values. The ratio K^1/K^2 is interesting—in most datasets we found that an asymmetric value performs better, e.g., the result of setting $K^1 = K^2 = 10$ is worse than $K^1 = 20, K^2 = 5$.

5.3 Object Arrangement

We finally considered the task of learning object arrangement in human scenes, using the dataset in [18]. It contains 3D models for 20 scenes such as living rooms, kitchens and offices, and 19 different object categories. Each room was manually labeled with arrangements of multiple objects. We considered two learning scenarios: placing new objects that are not in the test room and placing in an empty room. We performed 5-fold cross validation on 20 rooms and evaluated the predicted arrangements based on the location difference and height difference from the labels. We compared our hybrid M^3 model (with one DPMM for human poses and one finite mixture model for object affordances) against both a finite mixture model and a single DPM. Results are shown in Table 1. Our method not only predicts arrangements closer to the ground truth but also places relevant but different type of objects together due to it allows objects with different affordances share the same human pose.

6 Conclusion

In this paper, we presented the multidimensional membership mixture (M^3) models which consists of multiple independent mixture models. Each data point is generated from a set of mixture components jointly, designated by its multidimensional membership. We derived three instantiations of M^3 models—infinite, finite and hybrid M^3 . The infinite M^3 model uses multiple Dirichlet processes as the prior of memberships while the finite M^3 is built upon two LDAs. In both models, we introduced a tunable sharing parameter to increase its robustness in both sharing and no-sharing situations. The challenge in inference is addressed by Gibbs sampling and variational inference. We applied M^3 models on topic modeling. Compared to the baselines, our model demonstrated its ability in achieving better performance with fewer topics and in learning orthogonal topics. We also verified our model in the application of learning object arrangements.

References

- [1] D. Blei. Introduction to probabilistic topic models. *Communications of the ACM*, pages 1–16, 2011.
- [2] D. Blei and J. Lafferty. A correlated topic model of science. *The Annals App Stats*, 1(1):17–35, 2007.
- [3] D. Blei, A. Ng, and M. Jordan. Latent dirichlet allocation. *JMLR*, 3:993–1022, 2003.
- [4] L. Cao and L. Fei-Fei. Spatially coherent latent topic model for concurrent segmentation and classification of objects and scenes. In *ICCV*, 2007.
- [5] T. Chen, N. Zhang, T. Liu, and Y. W. K.M. Poon. Model-based multidimensional clustering of categorical data. *Artificial Intelligence*, 176:2246–2269, 2012.
- [6] A. Dai and A. Storkey. The grouped author-topic model for unsupervised entity resolution. *ICANN*, 1:241–249, 2011.
- [7] P. Das, R. Srihari, and Y. Fu. Simultaneous joint and conditional modeling of documents tagged from two perspectives. In *CIKM*, 2011.

VS+AP	VS+CN	VS+SP
parameter	response	force
measure	murray	digits
subthreshold	receptive	bifurcation
versions	lower	brain
tuned	type	dimension
bound	statistical	realized
obtain	bifurcation	electrodes
work	work	response
algorithms	section	cells
analysis	features	algorithms
images	neuron	form
achieved	problems	rate
form	obtained	low
local	images	local

Figure 7: Topics of VS combined with three other sections found by our finite M^3 model: top seven words (ranked by weight) of one topic from each dimension ($K^1 = 10, K^2 = 2$) is listed. Topics from first dimension are section-specific and different from each other while the second dimension contains popular terms in NIPS and the topics in it do not change much.

Table 1: Results of learning object arrangements evaluated by the difference in location and height (in meter).

	new object		empty room	
	location	height	location	height
FMM	1.59	0.16	1.74	0.20
DP	1.65	0.11	2.01	0.28
M^3	1.44	0.09	1.63	0.11

- [8] S. Deerwester, S. Dumais, G. Furnas, T. Landauer, and R. Harshman. Indexing by latent semantic analysis. *Journal of the American society for information science*, 41(6):391–407, 1990.
- [9] C. Ding, T. Li, and W. Peng. On the equivalence between non-negative matrix factorization and probabilistic latent semantic indexing. *CSDA*, 52(8):3913–3927, 2008.
- [10] H. Grabner, J. Gall, and L. J. V. Gool. What makes a chair a chair? In *CVPR*, 2011.
- [11] D. Griffiths and M. Tenenbaum. Hierarchical topic models and the nested chinese restaurant process. In *NIPS*, 2004.
- [12] T. Griffiths and M. Steyvers. Finding scientific topics. *PNAS*, 101(Suppl 1):5228, 2004.
- [13] T. Griffiths, M. Steyvers, D. Blei, and J. Tenenbaum. Integrating topics and syntax. In *NIPS*, 2004.
- [14] A. Gupta, S. Satkin, A. Efros, and M. Hebert. From 3D scene geometry to human workspace. In *CVPR*, 2011.
- [15] T. Hofman and J. Puzicha. Latent class models for collaborative filtering. In *IJCAI*, 1999.
- [16] T. Hofmann. Probabilistic latent semantic indexing. In *SIGIR*, pages 50–57, 1999.
- [17] A. Jalali, P. Ravikumar, S. Sanghavi, and C. Ruan. A dirty model for multi-task learning. In *NIPS*, 2010.
- [18] Y. Jiang, M. Lim, and A. Saxena. Learning object arrangements in 3d scenes using human context. In *ICML*, 2012.
- [19] R. Jin, L. Si, and C. Zhai. A study of mixture models for collaborative filtering. *Information Retrieval*, 9(3):357–382, 2006.
- [20] D. Kim and E. Sudderth. The doubly correlated nonparametric topic model. In *NIPS 24*, 2011.
- [21] S. Kim and E. Xing. Tree-guided group lasso for multi-task regression with structured sparsity. In *ICML*, 2010.
- [22] C. Li, A. Saxena, and T. Chen. θ -MRF: Capturing spatial and semantic structure in the parameters for scene understanding. In *NIPS*, 2011.
- [23] L. Li, C. Wang, Y. Lim, D. Blei, and L. Fei-Fei. Building and using a semantic visual image hierarchy. In *CVPR*, 2010.
- [24] L.-J. Li, R. Socher, and L. Fei-Fei. Towards total scene understanding: classification, annotation and segmentation in an automatic framework. In *CVPR*, 2009.
- [25] S. Madeira and A. Oliveira. Biclustering algorithms for biological data analysis: a survey. *Computational Biology and Bioinformatics, IEEE/ACM Transactions on*, 1(1):24–45, 2004.
- [26] B. Marlin and R. Zemel. The multiple multiplicative factor model for collaborative filtering. In *ICML*, 2004.
- [27] Q. Mei, D. Cai, D. Zhang, and C. Zhai. Topic modeling with network regularization. In *WWW*, 2008.
- [28] T. Minka and J. Lafferty. Expectation-propagation for the generative aspect model. In *UAI*, 2002.
- [29] L. Montesano, M. Lopes, A. Bernardino, and J. Santos-Victor. Learning object affordances: From sensory–motor coordination to imitation. *Robotics, IEEE Transactions on*, 24(1):15–26, 2008.
- [30] R. Nallapati, A. Ahmed, E. Xing, and W. Cohen. Joint latent topic models for text and citations. In *KDD*, 2008.
- [31] R. Neal. Markov chain sampling methods for dirichlet process mixture models. *J comp graph statistics*, 9(2):249–265, 2000.
- [32] D. Newman, E. Bonilla, and W. Buntine. Improving topic coherence with regularized topic models. In *NIPS*, 2011.
- [33] K. Nigam, J. Lafferty, and A. McCallum. Using maximum entropy for text classification. In *IJCAI workshop on machine learning for information filtering*, 1999.
- [34] D. P. Putthividhya, H. T. Attias, and S. Nagarajan. Independent factor topic models. In *ICML*, 2009.
- [35] M. Ranzato, A. Krizhevsky, and G. E. Hinton. Factored 3-way restricted boltzmann machines for modeling natural images. In *AISTATS*, 2010.
- [36] M. Rosen-Zvi, T. Griffiths, M. Steyvers, and P. Smyth. The author-topic model for authors and documents. In *UAI*, 2004.
- [37] E. Savia, K. Puolamaki, and S. Kaski. Latent grouping models for user preference prediction. *Mach Learn*, 74(1):75–109, 2009.
- [38] L. Si and R. Jin. Flexible mixture model for collaborative filtering. In *ICML*, 2003.
- [39] M. Steyvers and T. Griffiths. Probabilistic topic models. *Handbook of latent semantic analysis*, 427(7):424–440, 2007.
- [40] E. Sudderth, A. Torralba, W. Freeman, and A. Willsky. Describing visual scenes using transformed dirichlet processes. In *NIPS 18*, 2006.
- [41] Y. Teh, M. Jordan, M. Beal, and D. Blei. Hierarchical dirichlet processes. *J American Stat Association*, 101(476):1566–1581, 2006.
- [42] Y. Teh, D. Newman, and M. Welling. A collapsed variational bayesian inference algorithm for latent dirichlet allocation. In *NIPS 19*, 2007.
- [43] Y. W. Teh. Dirichlet process. *Encyclopedia of Machine Learning*, pages 280–287, 2010.
- [44] H. Wallach. Topic modeling: beyond bag-of-words. In *ICML*, pages 977–984, 2006.
- [45] C. Wang, D. Blei, and L. Fei-Fei. Simultaneous image classification and annotation. In *CVPR*, 2009.
- [46] X. Wang, X. Ma, and W. Grimson. Unsupervised activity perception in crowded and complicated scenes using hierarchical bayesian models. *T-PAMI*, 31(3):539–555, 2009.
- [47] S. Williamson, C. Wang, K. A. Heller, and D. M. Blei. Focused topic models. In *NIPS Workshop on Applications of Topic Models: Text and Beyond*, 2009.